

**Zeitschrift:** Schweizerische mineralogische und petrographische Mitteilungen = Bulletin suisse de minéralogie et pétrographie  
**Band:** 62 (1982)  
**Heft:** 1  
  
**Artikel:** K/Ar and  $^{40}\text{Ar}/^{39}\text{Ar}$  age resolution from illites of the Trias of Maulls; mesozoic cover of the Austroalpine basement, Eastern Alps (South Tyrol)  
**Autor:** Hammerschmidt, Konrad  
**DOI:** <https://doi.org/10.5169/seals-47965>

### **Nutzungsbedingungen**

Die ETH-Bibliothek ist die Anbieterin der digitalisierten Zeitschriften auf E-Periodica. Sie besitzt keine Urheberrechte an den Zeitschriften und ist nicht verantwortlich für deren Inhalte. Die Rechte liegen in der Regel bei den Herausgebern beziehungsweise den externen Rechteinhabern. Das Veröffentlichen von Bildern in Print- und Online-Publikationen sowie auf Social Media-Kanälen oder Webseiten ist nur mit vorheriger Genehmigung der Rechteinhaber erlaubt. [Mehr erfahren](#)

### **Conditions d'utilisation**

L'ETH Library est le fournisseur des revues numérisées. Elle ne détient aucun droit d'auteur sur les revues et n'est pas responsable de leur contenu. En règle générale, les droits sont détenus par les éditeurs ou les détenteurs de droits externes. La reproduction d'images dans des publications imprimées ou en ligne ainsi que sur des canaux de médias sociaux ou des sites web n'est autorisée qu'avec l'accord préalable des détenteurs des droits. [En savoir plus](#)

### **Terms of use**

The ETH Library is the provider of the digitised journals. It does not own any copyrights to the journals and is not responsible for their content. The rights usually lie with the publishers or the external rights holders. Publishing images in print and online publications, as well as on social media channels or websites, is only permitted with the prior consent of the rights holders. [Find out more](#)

**Download PDF:** 10.08.2025

**ETH-Bibliothek Zürich, E-Periodica, <https://www.e-periodica.ch>**

## **K/Ar and $^{40}\text{Ar}/^{39}\text{Ar}$ Age Resolution from Illites of the Trias of Mault; Mesozoic Cover of the Austroalpine Basement, Eastern Alps (South Tyrol)**

by *Konrad Hammerschmidt\**

### **Abstract**

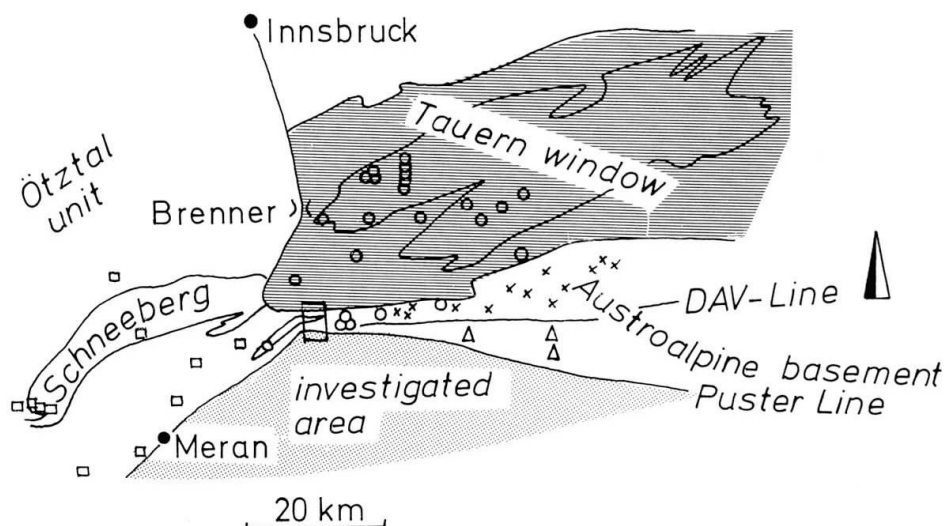
K/Ar and  $^{40}\text{Ar}/^{39}\text{Ar}$  isotope investigations were carried out on a slate from the so-called Trias of Mault in the Eastern Alps, the metamorphic grade of which reached the beginning of the greenschist facies. The  $^{40}\text{Ar}/^{39}\text{Ar}$  analysis revealed two mineral components in the grain size fraction 2–6  $\mu$ : one component must be considered as a detrital mica and the other component as a newly formed illite, which has lost 15% of its Ar (rad) since its formation about  $35 \pm 5$  Ma ago. The metamorphic grade at the beginning of the greenschist facies was insufficient to reset the  $^{40}\text{Ar}/^{39}\text{Ar}$  age spectrum of an illite (2–6  $\mu$ ) completely.




### **Introduction**

The so-called Trias of Mault – south of Innsbruck in the Italian part of the Eastern Alps – is situated in the Austroalpine basement (fig. 1) and consists of rocks of Permian and Triassic age. At this location the Austroalpine basement itself is only two kilometers thick and is delimited by the Tauern window (Schieferhülle) in the north (fig. 2). In rocks from the core of the Tauern window many investigators have determined Rb/Sr and K/Ar ages around 15 to 20 Ma (BESANG et al., 1968, JÄGER et al., 1969, SATIR, 1975), and in the Obere Schieferhülle Rb/Sr and K/Ar biotite and white mica ages around 16 to 18 Ma (HAMMERSCHMIDT, 1980). In the south the Austroalpine basement is separated from the Hercynian granite of Brixen (BORSI et al., 1972) by a tectonic line, the Puster line. Until now it is unclear where the Iffing intrusion is situated, either in the south of the Puster line or in the north (fig. 2). Another tectonic line, the Defreggen-Antholz-Valles line (DAV-line) divides the Austroalpine basement into two units. North of the DAV-line BORSI et al. (1978) and HAMMERSCHMIDT

---

\* Abteilung für Isotopengeologie, Erlachstrasse 9a, CH-3012 Bern.  
Present address: Physikalisches Institut, Sidlerstrasse 5, CH-3012 Bern.



-  Central gneisses and Penninic nappes
-  Austroalpine basement
-  Southern alps

#### Rb/Sr biotite ages from literature

|   |           |    |
|---|-----------|----|
| ○ | 15 - 20   | Ma |
| x | 20 - 30   | Ma |
| □ | 70 - 90   | Ma |
| △ | 270 - 300 | Ma |

Fig. 1 The age regimes at the southwestern part of the Tauern window. The age distribution are from the literature: BESANG et al., 1968; BORSI et al., 1973; W. FRANK et al., 1977; HAMMERSCHMIDT, 1981; JÄGER et al., 1969; SATIR, 1975.

(1981) have found Rb/Sr biotite and white mica ages from 17 to 30 Ma. South of the DAV-line only Hercynian biotite ages have been reported until now (BORSI et al., 1973, 1978). West of the Trias of Mault SATIR (1975) has obtained Rb/Sr biotite and muscovite ages around 80 Ma both within the Schneeberg unit and to the south of it in the crystalline basement.

The Trias of Mault is situated where these three age regimes meet, and consists of sericitic schists, phyllites, limestones and dolomites with Ladinian fossils (SCHINDLMAYER, 1968). The Permomesozoic sediments of the Trias of Mault record the Alpidic, metamorphic history exclusively. Structurally the Trias of Mault is a wedged syncline. The presence of clay films, quartz and carbonate mobilisation and a well developed cleavage indicate that the Trias of Mault has undergone low grade metamorphism, although the exact grade is unclear.

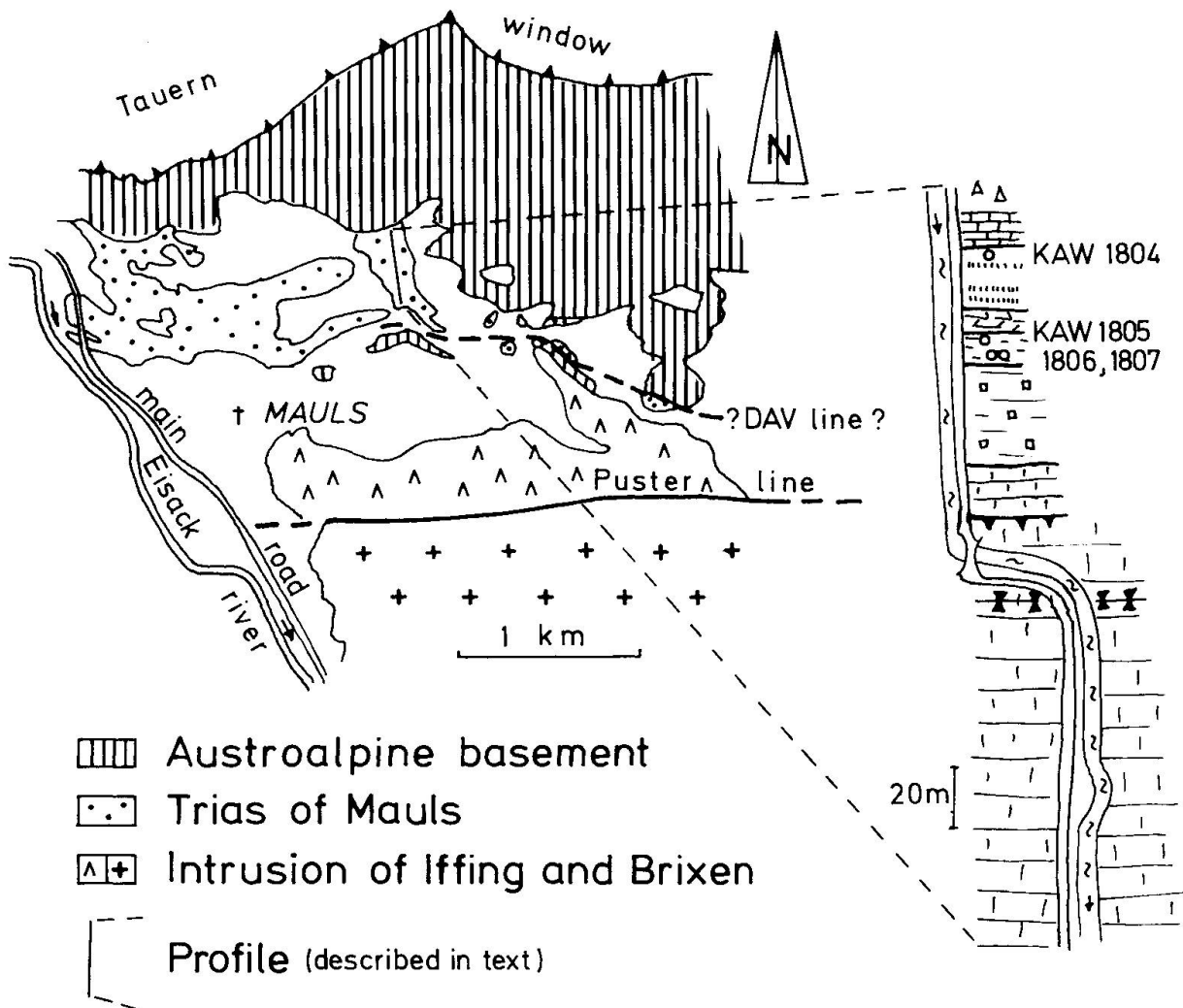


Fig. 2 The Trias of Mauls in the Austroalpine basement (after SCHINDLMAYR, 1968). The profile sketch shows the sample location.

If any Alpidic influence (e.g. metamorphism) was high enough, this will be detected by geochronological methods. As it is already mentioned above, the mineral ages of the Austroalpine basement obviously correspond to tectonic units, separated by faults (fig. 1). The Trias of Mauls should have illite ages in the same range as one of the crystalline units. If there is any age discrepancy, one has to consider an allochthonous position (thrust) for the Trias of Mauls. Therefore it is of interest to decide to which unit the Trias of Mauls belongs. For the relationship between the Mesozoic and the crystalline rocks there are four possibilities:

- 1) The Trias of Mauls is part of the northern crystalline block and was influenced by relatively low grade Alpidic metamorphism, the climax of which may be dated by the illites.

- 2) The Trias of Mauls is part of the southern block overlying its Hercynian basement. As such no Alpidic metamorphism should have influenced these rocks and the expected age of the illite will be near the time of its sedimentation. The DAV-line would be situated north of the Trias of Mauls in this case.
- 3) The Trias of Mauls belongs to the western part of the Austroalpine basement where the mica ages record the 80 Ma eoalpidic phase, evidenced by the Schneeberg unit results (SATIR, 1975).
- 4) If the metamorphic temperatures were high enough in Tertiary times, e.g.  $350^{\circ} \pm 50^{\circ}\text{C}$  according to PURDY and JÄGER (1976), cooling ages would be expected, as W. FRANK et al. (1977) have found in the southwestern continuation of the Trias of Mauls, the so-called Trias of Stilfes. The grain size fractions smaller than  $2\ \mu$  from Permomesozoic sericitic schists, where detrital micas are present, give Alpidic cooling ages from 15 to 22 Ma.

The investigations were also carried out to test the age resetting of illite under the metamorphic conditions found at the beginning of greenschist facies. This may be best done with the  $^{40}\text{Ar}/^{39}\text{Ar}$  method, which permits resolution between excess and loss of argon (LANPHERE and DALRYMPLE, 1971; HARRISON and MCDUGALL, 1980; E. FRANK and STETTLER, 1981).

### Problems in dating illites

One of the problems in dating the age of very low grade metamorphism is to find minerals which have had a zero age coincident with the metamorphic event. Illites, K-bearing white micas of diagenetic and anchimetamorphic origin, usually with a deficit of potassium in the unit cell, appear suitable for K/Ar dating (HURLEY et al., 1961; BAILEY et al., 1962; HUNZIKER, 1979).

Two possibilities must be considered. Firstly if clay minerals were formed during sedimentation and subsequently have suffered no loss of radiogenic products, these minerals will approximately date the age of sedimentation (i.e. glauconies, ODIN, 1982). However if these minerals underwent a metamorphism liberating all the radiogenic products produced until that time, then the results obtained from these minerals give the age of metamorphism.

Secondly, if in the sediments diagenetic clay minerals and a detrital component (e.g. illite and muscovite) exist, mixing ages occur ranging between the age of sedimentation and the age of the detrital component. With increasing metamorphism the clay minerals change to well defined phengites and/or muscovites. If the two mica components lose all their radiogenic products accumulated between the time of formation and the time of successive metamorphism,

then the mixture of former clay minerals and detrital muscovite date the approximate time of metamorphism.

The interpretation of illite ages depends upon several mineralogical criteria:

### 1) The crystallinity index

The crystallinity index (KÜBLER, 1967) is determined by x-ray diffractometry on the grain size fraction  $< 2\ \mu$  by measuring the width of the d(001) peak at half height in millimeters. A value greater than 7.5 indicates diagenesis, a value between 7.5 and 4.0 anchimetamorphism, and a value less than 4.0 greenschist facies. HUNZIKER (1979, p. 65) considers that under certain conditions, "... recrystallized illites can be used safely to determine the age of metamorphism from the transition anchizone-epizone up to higher degrees of metamorphism". If, for the same sample the illite crystallinity index for grain size fractions  $< 20\ \mu$  tends towards lower values, the presence of detrital mica must be considered.

### 2) The polymorphism of illite

During diagenesis 1M and 1Md polymorphs of illite are formed, which change into the 2M modification at anchimetamorphism (FREY, 1978; DUNOYER, 1970). According to HUNZIKER (1979) illite loses all its radiogenic products, and the radiogenic clock is restarted with the transition from the 1M/1Md to the 2M<sub>1</sub> structure with the metamorphism. If there is a profile from diagenesis to higher metamorphic grade within the same stratum and in the diagenetic sediments 1M and 2M polymorphs of illite are present, the 2M polymorph must be considered as detrital component. In a higher grade of metamorphism only 2M polymorphs exist and it is uncertain whether all the 2M polymorphs of detrital origin have lost their radiogenic argon at the time of metamorphism. If the composition of the nonmetamorphosed educt is unknown, it could be possible that newly formed 2M<sub>1</sub> micas are mixed with 2M<sub>1</sub> micas of detrital origin, which obviously could result in geologically meaningless conclusions.

As HURLEY (1966) has mentioned, and E. FRANK and STETTLER (1979) have established in a profile at one stratum from the Doldenhorn to Verampio (Swiss alps), the complete conversion of 1Md to 2M<sub>1</sub> illite indicates only the beginning of total outgassing of all pre-existing radiogenic argon.

### 3) The chemical composition of illite

With the increase of metamorphic processes in sediments the following mineral sequence has been found: smectite – smectite/illite – illite – muscovite (DUNOYER, 1970; HOWER et al., 1971). The chemical composition of the illite may be

estimated using the  $d(060, \bar{3}31)$  spacing: At the tetrahedral layer of the muscovite the ratio Si/Al is 6:2 and this ratio changes to 7:1 for phengite. The more phengitic the illites, the higher are the values of the  $d(060, \bar{3}31)$  spacings. To maintain the charge balance, Al from the octahedral sites must be replaced by Mg and/or Fe.

This work was carried out to test not only regional geological hypotheses but also to contribute to the understanding of K/Ar ages in low metamorphic terranes.

### **Geology of the samples**

#### ***Geological profile of the sample locality***

In the Sengesbach gorge the following profile was recorded from south to north (fig. 2, with sample locations):

- 150 m calcic and dolomitic marbles with hornstone layers, thickly bedded, folded in a large syncline with a wavelength of about 20 m; followed by a fault
- 20 m dark massive calcic marbles
- 35 m cellular dolomite
- 10 m dark coloured, red weathered slates, with a cleavage parallel to the bedding; location of samples KAW 1805, 1806, 1807
- 8 m massive dark dolomite
- 20 m dark coloured slates, with three 20 cm thick dolomitic beds; sample KAW 1804
- 12 m grey dolomite.

The contact with the Austroalpine basement is covered by detritus. The dolomites and marbles at the southern end of the Sengesbach gorge are of Ladinian age according to palaeontological evidence (SCHINDLMAYR, 1968). The slates exist only at this location and are equivalent to the Raibler beds (SCHINDLMAYR, 1968).

### **Mineralogy of the samples**

#### ***Mineral separation***

Only slates from the Mesozoic part of the Trias of Maultal were investigated. About 500 gr of each ground rock sample were separated by sedimentation in

Atterberg cylinders. Any carbonate, if present in the whole rock sample, was dissolved in 5% acetic acid and subsequently the mica fraction was thoroughly rinsed with distilled water. The mineral fraction smaller than  $2\ \mu$  was quantitatively removed before separating the next larger grain size (e.g.  $2\text{--}6\ \mu$ ). Usually in the size fraction  $2\text{--}20\ \mu$  there are still about 5% of the grain size fraction  $< 2\ \mu$ . The original grain size is in the order of  $2\ \mu$  to  $20\ \mu$ . In respect to the sedimentation method of the samples the mineral agglomeration are not aliquots *sensu strictu*.

#### *X-ray analyses*

The illite crystallinity index was measured according to KÜBLER (1967) using standardized conditions (Cu-tube at 40 KV/22 mA) as described above. The basal reflections  $d(001)$  determining the paragonite molecule were measured with a goniometer speed of  $0.125^\circ/\text{hour}$ . The  $d(hkl)$  spacings were analyzed by Guinier camera technique with a Fe-tube at 40 KV/22 mA using quartz as an internal standard. The reproducibility of several independent measurements was better than  $0.0010\ \text{\AA}$ . The relative amount of mica in the separated mineral fractions was estimated by comparison with precisely known mixtures of minerals.

#### *The mineral composition of the slates*

The mineral compositions of the slates (whole rock) and of the grain size fraction  $< 2\ \mu$  and  $2\text{--}20\ \mu$  are given in table 1. The relative amounts of illite and chlorite are normalized to 100.

In the whole rock samples quartz is always present, and in addition K-feldspar and albite may appear, and occasionally calcite and dolomite are found. Chlorite appears only in the samples KAW 1806 and 1807. The relative distribution of illite and chlorite are different in each grain size fraction. In the whole rock sample KAW 1807 the ratio illite/chlorite is about 2.4. In the  $2\text{--}20\ \mu$  fraction the ratio changes to 1.3, in the  $< 2\ \mu$  fraction to 4.2. It seems that the amount of illite is reduced relative to chlorite in the grain size fraction  $2\text{--}20\ \mu$  and again enriched in the grain size  $< 2\ \mu$ . In the  $< 2\ \mu$  fraction of sample KAW 1804 besides quartz only illite was found. The potassium content of the samples decreases with increasing amounts of quartz (5–20%).

The crystallinity index of the illite from these samples varies between 3.8 and 4.9 for the  $< 2\ \mu$  fraction and between 3.3 and 4.0 for the  $2\text{--}20\ \mu$ . The differences are very small, but it seems possible that two different white micas are present. The amount of detrital mica would have to be less than 5%, otherwise the crystallinity indices would show decreasing values.

The crystallinity index shows also that the slates of the Trias of Mauls under-

went a metamorphism nearly reaching the beginning of greenschist grade. Only the  $2M_1$  polymorph of mica was found.

The composition of micas in the solid solution between muscovite (Si:Al = 6:2) and phengite (Si:Al = 7:1) was estimated from the  $d(060, \bar{3}31)$  spacing, as described above. The spacing ranges from 1.5036 Å to 1.5075 Å in the  $< 2 \mu$  fraction, and that of the 2–20  $\mu$  fraction varies from 1.5021 to 1.5065 Å, as shown in table 1. These high values indicate illite of phengitic composition. To estimate the chemical composition of illite in terms of a soluble paragonite component, the  $d(002)$  spacing was used (YODER and EUGSTER, 1955; BURNHAM and RADOSLOVICH, 1964; GUEVEN, 1967). According to a correlation of ZEN E-AN and ALBEE (1964) the illites investigated here have between 4 and 25 mol-% paragonite (table 1). Because no paragonite in paragenesis with illite was found in the investigated samples, only a lower limit may be estimated for metamorphic temperatures at around the beginning of the greenschist facies. The estimated chemical compositions of the samples point to a development of the micas from clay minerals to phengites, which is normally found in sedimentary rocks of prograde metamorphism. From the mineralogical investigations it is uncertain whether the slates of the Trias of Mauls contain detrital micas.

Table 1 Mineralogical data of the investigated samples.

| KAW Nr.               | Mica       | Chl | Q | Kf  | Ab       | Cc | Dol | IC  | d<br>(060, $\bar{3}31$ ) | d<br>(002) | Mol-% Pa |
|-----------------------|------------|-----|---|-----|----------|----|-----|-----|--------------------------|------------|----------|
| -----                 |            |     |   |     |          |    |     |     |                          |            |          |
| Whole rock            |            |     |   |     |          |    |     |     |                          |            |          |
| 1804                  | 100        |     | + |     |          | +  | +   |     |                          |            |          |
| 1805                  | 100        |     | + | +   | +        | +  |     |     |                          |            |          |
| 1806                  | 75         | 25  | + | +   | +        | +  |     |     |                          |            |          |
| 1807                  | 71         | 29  | + | +   | +        |    |     |     |                          |            |          |
| -----                 |            |     |   |     |          |    |     |     |                          |            |          |
| Fraction 2 – 20 $\mu$ |            |     |   |     |          |    |     |     |                          |            |          |
| 1804                  | 100        |     | + |     | +        | +  | +   | 3.3 | 1.5021                   | 10.040     |          |
| 1805                  | 100        |     | + | +   | +        |    |     | 4.0 | 1.5050                   | 10.052     |          |
| 1806                  | 75         | 25  | + | +   |          |    |     | 3.8 | 1.5065                   | 10.017     | 4.0      |
| 1807                  | 57         | 43  | + | +   |          |    |     | 3.9 | 1.5058                   | 10.063     |          |
| -----                 |            |     |   |     |          |    |     |     |                          |            |          |
| Fraction $< 2 \mu$    |            |     |   |     |          |    |     |     |                          |            |          |
| 1804                  | 100        |     | + |     |          |    |     | 3.8 | 1.5036                   | 9.9608     | 17.0     |
| 1805                  | 100        |     | + |     |          |    |     | 4.9 | 1.5044                   | 9.9720     | 14.5     |
| 1806                  | 81         | 19  | + |     |          |    |     | 4.5 | 1.5075                   | 10.057     |          |
| 1807                  | 81         | 19  | + |     |          |    |     | 4.4 | 1.5067                   | 9.9273     | 24.9     |
| -----                 |            |     |   |     |          |    |     |     |                          |            |          |
| Chl                   | chlorite   |     |   | Ab  | albite   |    |     | Pa  | paragonite               |            |          |
| Q                     | quartz     |     |   | Cc  | calcite  |    |     | IC  | crystallinity index      |            |          |
| Kf                    | k-feldspar |     |   | Dol | dolomite |    |     |     |                          |            |          |

### Isotope investigations

#### *K/Ar isotope analyses (conventional method)*

The isotope composition and absolute amounts of argon were measured on a mass spectrometer (Varian MAT GD 150), using a  $^{38}\text{Ar}$ -spike (from Prof. Clusius, Zurich) calibrated against the Be 4 M muscovite standard of Bern. Further analytical details are described by PURDY (1972) and HUNZIKER (1974). The  $2\sigma$ -error on the argon isotope determination was estimated as 3%, including errors of spike concentration, of air argon ratio and of the standard (HUNZIKER, 1974).

Potassium concentrations were measured with a Beckmann flame photometer, using a hydrogen-oxygen flame. The samples were dissolved with a mixture of hydrofluoric and perchloric acid. To avoid matrix effects the evaporated samples were diluted with 0.1 n hydrochloric acid to less than 10 ppm potassium. Two aliquots of each sample solution were measured and compared with calibrated potassium solutions. The constants recommended by STEIGER and JÄGER (1977) were used for age calculation. On the standard Be 4 M the  $2\sigma$ -error has been determined as 0.5% (PURDY and JÄGER, 1976).

#### *$^{40}\text{Ar}/^{39}\text{Ar}$ isotope analyses*

The 2–6  $\mu$  fraction of sample KAW 1804 was irradiated using fast neutrons with five other micas and six terrestrial monitors (Be 4M) at the Kernforschungszentrum Karlsruhe, BRD. Between 8 and 20 mg of samples and monitors were enveloped in high purity Al-foils, separately packaged into Al-containers which were then evacuated to a pressure of less than  $10^{-2}$  mbar. After careful filling with nitrogen to slightly more than 1025 mbar, the Al-containers were cold-welded and then enclosed in a 0.6 mm Cd shielded Harwell capsule. To monitor the horizontal and vertical variation of the neutron fluence ( $E > 0.1$  MeV) small Ni-ribbons were fixed outside each container. The  $^{58}\text{Co}$ -activities from the  $^{58}\text{Ni}$  (n, p)  $^{58}\text{Co}$  reaction were measured at Karlsruhe with a  $2\sigma$  relative statistical error of 3‰ (priv. comm. Mr. Rottmann). The fast neutron fluence gradient over all samples was found to be  $\leq 2.5\%$  and this was corrected for by normalizing to the mean value. The integrated mean fluence for neutrons with energies above 0.1 MeV was  $6.0 \cdot 10^{17} \text{ n}_f\text{cm}^{-2}$ . After irradiation, the samples were baked out at 130°C for 24 hours in the extraction system, degassed stepwise and the argon isotope composition for each step measured on-line with the double magnetic mass spectrometer assembly at the Physikalisches Institut in Bern (SCHWARZMÜLLER, 1970). The reciprocal sensitivity of the mass spectrometer was determined as  $(5.691 \pm 0.079) \cdot 10^{-12} \text{ cm}^3 \text{ STP } ^{40}\text{Ar}/\text{mV}$  with an argon standard.

All ratios were corrected for discrimination (0.0085 per amu). Extraction

Table 2 Extraction line blank and mass spectrometer background at various temperatures given in  $^{40}\text{Ar}$ -equivalent.

| Temp. \ Mass | 40  | 39   | 38<br>in $10^{-12} \text{ cm}^3$ | 37<br>per step | 36  | 35   |
|--------------|-----|------|----------------------------------|----------------|-----|------|
| 600°C        | 250 | 0.85 | 0.85                             | 0.2            | 1.1 | 0.22 |
| 1100°C       | 280 | 0.91 | 0.91                             | 0.2            | 1.1 | 0.22 |
| 1400°C       | 540 | 0.90 | 0.95                             | 0.25           | 1.9 | 0.25 |

blanks (that is the background of the mass spectrometer and the contribution of the extraction line) increased typically from lower to higher temperature steps. Table 2 gives a summary of the blanks in  $^{40}\text{Ar}$ -equivalents. A computer program by GUGGISBERG (1974) from the Physikalisches Institut in Bern was adapted and used for calculations. All the ratios were corrected for blanks, discrimination, Ar interferences from neutron reactions with Ca and K (table 4), and also for neutron fluence inhomogeneity.

The radioactive decay of  $^{37}\text{Ar}$  and  $^{39}\text{Ar}$  was taken into consideration using the following decay constants:  $\lambda_{37} = 0.01975 \text{ d}^{-1}$  and  $\lambda_{39} = 7.2 \cdot 10^{-6} \text{ d}^{-1}$ . After these corrections all  $^{36}\text{Ar}$  was considered to be atmospheric. This assumption is valid only if the volume of chlorine present in the mass spectrometer is negligible and therefore mass 35 (chlorine) was always measured. Even the maximum measured value of  $2.5 \cdot 10^{-13} \text{ cm}^3$   $^{40}\text{Ar}$ -equivalents for mass 35 may be neglected. The radiogenic argon component was calculated with the air ratio  $^{40}\text{Ar}/^{36}\text{Ar} = 295.5$ . For  $^{38}\text{Ar}$  an air correction was also made and the residual  $^{38}\text{Ar}$  is considered to originate from chlorine by the reaction  $^{38}\text{Cl} (n, \gamma \beta) ^{38}\text{Ar}$ .

The errors given in the table 4 correspond to the 95% confidence level and takes into account the following error sources: statistics of measurements, discrimination, blank (usually 20% for  $^{39}\text{Ar}$  and 30% for the other argon isotopes), interferences, reciprocal sensitivity, weight, and relative measurements of the neutron fluence.

## Results

### *Conventional K/Ar data*

The analytical data obtained with the conventional K/Ar method are listed in table 3. The "ages" of the  $< 2 \mu$  fraction range between 35 and 45 Ma and are generally younger than those of the 2–20  $\mu$  fraction which lie between 30 and 60 Ma. What is the geological meaning of these "ages"? Two interpretations appear possible:

Table 3 Potassium and argon analyses on slates of the grain size fraction smaller  $2\mu$ ,  $2-6\mu$  and  $2-20\mu$ .

| KAW Nr. | Grain size  | % K  | $^{40}\text{Ar}(\text{rad}) * 10^{-6}$<br>$\text{cm}^3 \text{ STP/gr}$ | Age in Ma      |
|---------|-------------|------|--|----------------|
| 1804    | $2\mu$      | 6.72 | 9.54   | $35.9 \pm 1.4$ |
| 1804*   |             |      | 9.74   | $36.9 \pm 1.4$ |
| 1805    | $2\mu$      | 6.53 | 10.83  | $41.9 \pm 2.4$ |
| 1806    | $2\mu$      | 5.73 | 9.89   | $43.6 \pm 2.0$ |
| 1807    | $2\mu$      | 5.83 | 10.38  | $44.9 \pm 1.7$ |
| 1804    | $2 - 6\mu$  | 5.80 | 9.96   | $44.1 \pm 1.8$ |
| 1804    | $2 - 20\mu$ | 5.12 | 8.15   | $40.5 \pm 1.3$ |
| 1804*   |             |      | 8.25   | $40.9 \pm 1.4$ |
| 1805    | $2 - 20\mu$ | 6.01 | 13.33  | $55.8 \pm 2.1$ |
| 1806    | $2 - 20\mu$ | 5.52 | 10.86  | $49.6 \pm 2.4$ |
| 1807    | $2 - 20\mu$ | 5.10 | 12.04  | $59.4 \pm 2.3$ |

\* repetition of Ar analysis

Firstly the ages may be mixed ages intermediate between the cooling ( $15-22\text{ Ma}$ ) and the  $80\text{ Ma}$  event. Secondly the  $< 2\mu$  fraction shows ages around  $40 \pm 5\text{ Ma}$  coincident with the climax of the Tauern metamorphism, suggested by SATIR (1975) between  $35$  and  $40\text{ Ma}$ .

Using the  $^{40}\text{Ar}/^{39}\text{Ar}$  analytical method it is possible to distinguish between such alternative hypotheses.

#### $^{40}\text{Ar}/^{39}\text{Ar}$ data

In a reactor a definable portion of  $^{39}\text{K}$  will be converted to  $^{39}\text{Ar}$  by irradiation with fast neutrons. Afterwards the argon is released from the sample in steps by heating at successively higher temperatures. The apparent age of each gas increment can be calculated from the  $^{40}\text{Ar}/^{39}\text{Ar}$  ratio. The results may be plotted to give a so-called age spectrum, a diagram of apparent ages versus cumulative fraction of  $^{39}\text{Ar}$  released (e.g. fig. 3).

If a mineral has been a closed system to potassium and argon since its formation, then the  $^{40}\text{Ar}/^{39}\text{Ar}$  ratio and therefore the age, should be constant in each temperature step. If the mineral system was disturbed by a geological event, then the age spectrum should be disturbed too, offering the possibility of distinguishing between excess argon (LANPHERE and DALRYMPLE, 1971; HARRISON and MCDUGALL, 1980), or argon loss induced during this geological event (E. FRANK and STETTLER et al., 1981).

As the sample KAW 1804 contains only illite and quartz with no chlorite, it was chosen for the  $^{40}\text{Ar}/^{39}\text{Ar}$  method, and to avoid recoil effects (HUNECKE and SMITH, 1976) the size fraction  $2-6\mu$  was selected, where the grain size is

Table 4  $^{40}\text{Ar}/^{39}\text{Ar}$  analysis of the sample KAW 1804, 2-6  $\mu$ .

| Temp °C | $^{40}\text{Ar}/^{36}\text{Ar}$ | $^{39}\text{Ar}/^{36}\text{Ar}$ | $^{39}\text{Ar}/^{37}\text{Ar}$ | $^{39}\text{Ar} \times 10^{-8}$<br>$\text{cm}^3 \text{ STP/g}$ | $^{40}\text{Ar}(\text{rad})/^{39}\text{Ar}(\text{K})$ | Age in Ma        |
|---------|---------------------------------|---------------------------------|---------------------------------|--|---|------------------|
| 475     | $306.0 \pm 6.0$                 | $27.05 \pm 0.70$                | $14.65 \pm 0.60$                | $1.130 \pm 0.035$  | $0.37 \pm 0.20$                                       | $1.9 \pm 0.9$    |
| 555     | $471.0 \pm 7.0$                 | $105.0 \pm 6.0$                 | $16.3 \pm 2.0$                  | $1.820 \pm 0.070$  | $1.790 \pm 0.080$                                     | $9.1 \pm 0.4$    |
| 610     | $504.0 \pm 8.0$                 | $74.6 \pm 3.0$                  | $12.61 \pm 0.40$                | $1.220 \pm 0.060$  | $3.02 \pm 0.15$                                       | $15.35 \pm 0.80$ |
| 670     | $634 \pm 25$                    | $124.0 \pm 6.0$                 | $17.90 \pm 0.50$                | $1.685 \pm 0.070$  | $2.98 \pm 0.10$                                       | $15.20 \pm 0.80$ |
| 720     | $1595 \pm 60$                   | $389 \pm 10$                    | $65.5 \pm 6.0$                  | $5.430 \pm 0.15$   | $4.145 \pm 0.080$                                     | $21.10 \pm 0.50$ |
| 790     | $3350 \pm 110$                  | $602 \pm 30$                    | $63.9 \pm 2.0$                  | $9.10 \pm 0.19$  | $5.690 \pm 0.090$                                     | $28.90 \pm 0.50$ |
| 850     | $4900 \pm 280$                  | $714 \pm 40$                    | $58.20 \pm 0.40$                | $65.4 \pm 1.4$   | $8.43 \pm 0.15$                                       | $42.60 \pm 0.80$ |
| 870     | $5685 \pm 330$                  | $766 \pm 40$                    | $47.40 \pm 1.00$                | $10.17 \pm 0.20$   | $9.60 \pm 0.15$                                       | $48.50 \pm 0.90$ |
| 890     | $3980 \pm 230$                  | $536 \pm 25$                    | $40.8 \pm 2.0$                  | $4.27 \pm 0.10$  | $10.10 \pm 0.20$                                      | $50.9 \pm 1.0$   |
| 920     | $2955 \pm 150$                  | $309 \pm 15$                    | $41.15 \pm 0.70$                | $3.210 \pm 0.070$  | $10.45 \pm 0.17$                                      | $52.70 \pm 1.0$  |
| 960     | $3565 \pm 170$                  | $308 \pm 15$                    | $44.8 \pm 2.45$                 | $2.810 \pm 0.060$  | $12.04 \pm 0.18$                                      | $60.6 \pm 1.1$   |
| 1020    | $1069 \pm 16$                   | $59.9 \pm 1.2$                  | $36.80 \pm 0.70$                | $2.548 \pm 0.050$  | $13.07 \pm 0.19$                                      | $65.7 \pm 1.2$   |
| 1060    | $1810 \pm 55$                   | $93.3 \pm 3.0$                  | $57.5 \pm 5.0$                  | $1.640 \pm 0.030$  | $16.53 \pm 0.25$                                      | $82.7 \pm 1.5$   |
| 1120    | $1366 \pm 40$                   | $26.0 \pm 1.0$                  | $11.6 \pm 1.4$                  | $0.224 \pm 0.004$  | $42.1 \pm 0.7$  | $203.5 \pm 4.0$  |
| 1840    | $425.0 \pm 6.0$                 | $5.42 \pm 0.10$                 | $2.30 \pm 0.40$                 | $0.202 \pm 0.004$  | $23.8 \pm 0.9$  | $117.7 \pm 4.2$  |
| Total   | $2580 \pm 120$                  | $348 \pm 18$                    | $49.25 \pm 1.9$                 | $110.9 \pm 2.2$  | $8.30 \pm 0.14$                                       | $42.01 \pm 0.80$ |

J value :  $0.002837 \pm 27$ 

rad : radiogenic

K : neutron produced from K only

 $\lambda = 5.543 \times 10^{-10} \text{ a}^{-1}$  (STEIGER and JÄGER, 1979)

Standard Be 4 M : K 8.70 + 0.05 % (PURDY and JÄGER, 1976)

t 18.5 + 0.2 Ma (FLISCH, 1981)

Correction for interferences:

 $^{36}\text{Ar}/^{37}\text{Ar}(\text{Ca}) = 2.7 \pm 0.2 \times 10^{-4}$  $^{38}\text{Ar}/^{37}\text{Ar}(\text{Ca}) = 6.0 \pm 2.0 \times 10^{-5}$  $^{39}\text{Ar}/^{37}\text{Ar}(\text{Ca}) = 6.8 \pm 0.2 \times 10^{-4}$  $^{40}\text{Ar}/^{37}\text{Ar}(\text{Ca}) = 3.0 \pm 3.0 \times 10^{-4}$  $^{38}\text{Ar}/^{39}\text{Ar}(\text{K}) = 1.4 \pm 0.3 \times 10^{-1}$  $^{40}\text{Ar}/^{39}\text{Ar}(\text{K}) = 6.0 \pm 2.0 \times 10^{-3}$ 

STETTLER et al., 1973

TURNER et al., 1973

MAURER, 1973

STETTLER et al., 1973

20–60 times greater than the range of recoiled argon. In addition, this grain size fraction of the sample consists of nearly pure illite.

The data of the fifteen temperature steps are listed in table 4. All the data used in this paper may be taken from this table or may be calculated by simple conversions.

The temperature steps increase from 475°C to 1840°C and the resulting apparent ages are plotted in an age spectrum diagram (fig. 3). The ages increase progressively from 1.9 to 203.5 Ma with a decrease in the last temperature step to 117.7 Ma. In addition the K/Ca ratio, calculated from the  $^{39}\text{Ar}/^{37}\text{Ar}$  ratio was plotted vs. the cumulatively released fraction of  $^{39}\text{Ar}$ . In the first four temperature steps (475°–670°C) the K/Ca ratio varies from 6.3 to 8.0, then it increases to about 30, and at 870°C the K/Ca ratio decreases slowly.

The age spectrum is separated into two parts. In the low temperature range the age curve is convex and passes into a concave curve at higher temperature. Notice that the temperature step of 850°C contains nearly 60% of the total  $^{39}\text{Ar}$  released: such a plateau-like step is produced by the expulsion of the OH-groups in the micas.

### Discussion

The spread of the conventional K/Ar ages, as well as the mineralogical data, point to a complex illite composition and history for sample KAW 1804.

In contrast, the  $^{40}\text{Ar}/^{39}\text{Ar}$  method permits the resolution of a complex history as seen in fig. 3. In interpreting the age spectrum it may be considered that either two distinct mineral phases with differing  $^{40}\text{Ar}$  retentivities or one mineral phase with two types of  $^{40}\text{Ar}$  retentivity (one lower and one higher) were degassed. The phase with low Ar retentivity is indicated at the lower temperature step with the resulting low apparent ages. The phase with high Ar retentivity may be seen at the high temperature steps, where the apparent ages increase to 200 Ma.

The low apparent age in the first temperature step (1.9 Ma) may be an artefact. At the corners of the small illite grains  $^{40}\text{Ar}(\text{rad})$  loss may occur through the preheating (< 150°C) in the reactor. The drop in the last temperature step from about 200 Ma to about 120 Ma may be explained by recoil (HUNECKE and SMITH, 1976).  $^{39}\text{Ar}$  in less retentive positions will be transferred to more highly retentive sites, resulting in smaller apparent ages.

In terms of mineralogy the low temperature phase corresponds to the newly formed illite. After its formation, at a maximum of 45 Ma ago, it lost  $^{40}\text{Ar}$  as indicated in the lower apparent ages given by the lower temperature steps. In contrast the high temperature phase could result from an old detrital mica overgrown by the newly formed illite, or from a separate, detrital mica phase, which

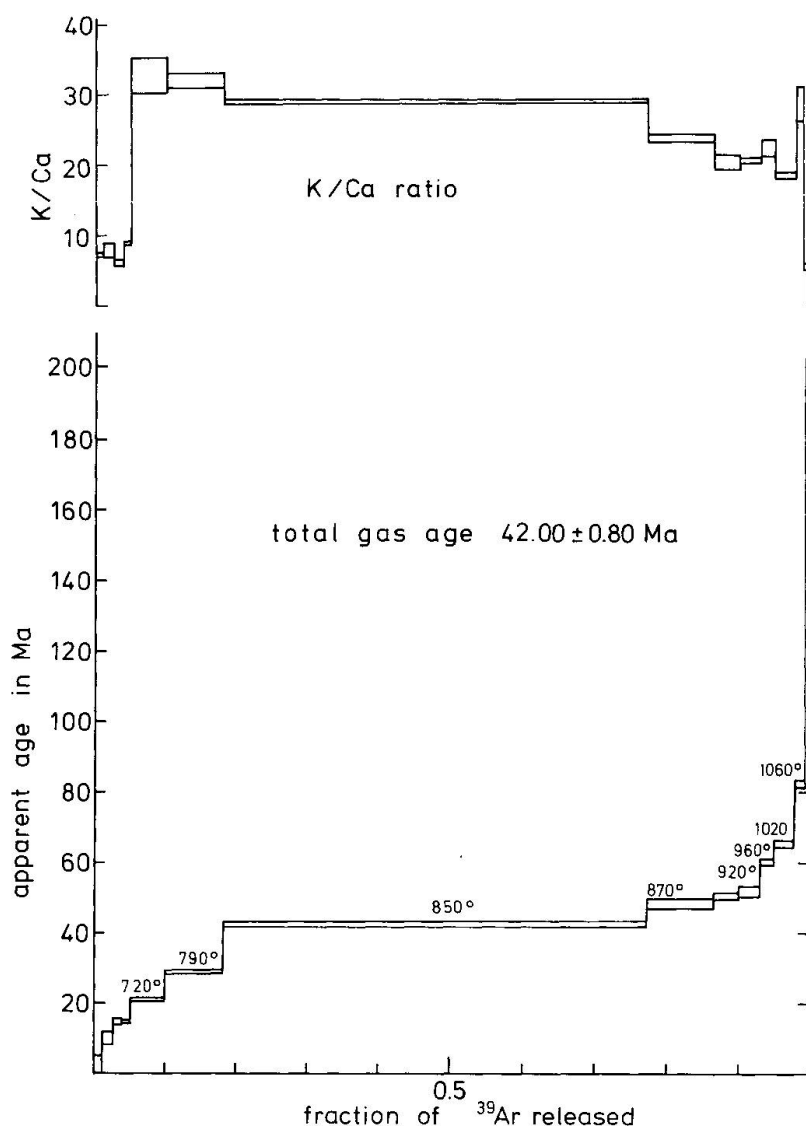


Fig. 3 The age spectrum of the slate KAW 1804, 2-6  $\mu$ .

causes the high apparent ages in the high temperature steps. Both possibilities would result in similar age spectra.

In estimating the influence of a possible old mica component the following model was considered. A 310 Ma old mica loses 60%, 80% and 90% respectively of its original  $^{40}\text{Ar}(\text{rad})$  content at 30 to 40 Ma (the climax of the Tauern metamorphism) shown as curves A, B and C in figure 4. A newly formed illite has a plateau age of  $35 \pm 5$  Ma and a 15% argon loss indicated by the dashed line D. Curves A, B and C are superimposed on D under the assumption that 95% of the mineral concentrate consists of newly formed mica and 5% is the old component and the diffusion parameters of the two components are equal. The detection limit of a detrital mica component by X-ray analysis is of the order of 5%. The corresponding mixture curves are labelled with "a", "b" and "c" re-

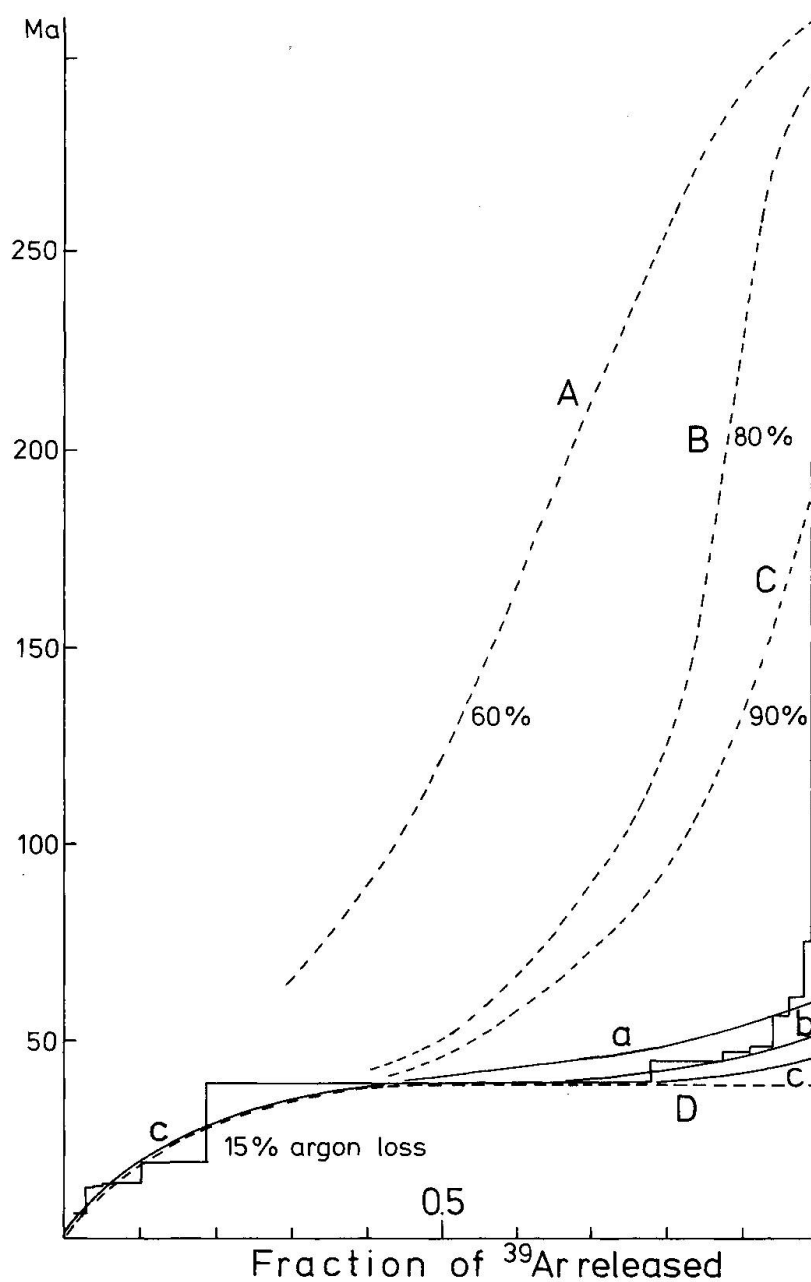


Fig. 4 The curves A, B and C represent a 60%, a 80% and a 90% radiogenic argon loss of a 310 Ma old mica. The staircase pattern is the measured age spectrum of the sample KAW 1804. The curve labelled with 15% argon loss documents a newly formed illite with a plateau age of about  $35 \pm 5$  Ma and a 15% argon loss. This curve and curve C were superimposed under the assumption that 95% of the newly formed illite is contributed to 5% of the old mica resulting in curve c and so on.

spectively in the figure 4. The assumptions and the theoretical gas loss were discussed by TURNER (1968).

The curves a, b and c do not show very good agreement with the measured spectrum (fig. 4). A better agreement between the measured and calculated age spectra would be obtained by linearly increasing the portion of the detrital component with each successive temperature step.

In the low temperature range the 15% gas loss of the newly formed illite subsequent to formation was calculated (curve D). This curve agrees very well with the measured one. Even a constant gas content (5%) from the old mica component (90% gas loss) to the newly formed illite does not change the curve drastically (see fig. 4).

The above mentioned gas loss, which the minerals had suffered during the geological history, was discussed for the  $^{40}\text{Ar}(\text{rad})$  component. However the gas loss for this sample may be considered a second way. The  $^{39}\text{Ar}$  produced in the reactor has the same diffusion behaviour during the stepwise heating experiment as the  $^{40}\text{Ar}(\text{rad})$  during the geological history.

The degassing curve is divided into two parts by the expulsion of the OH-groups in the 850°C temperature step. After this step a new homogeneous reservoir is considered. Therefore the  $^{39}\text{Ar}$  released from the step from 890°C to 1800°C is normalised to 100%, from which the activation energy (183 kJ/mol) and the diffusion constants at 150°, 200° and 300°C were calculated (tab. 5). For the low temperature steps the whole amount of the  $^{39}\text{Ar}$  of the sample is regarded as the driving force for diffusion (2. Fick law) and therefore normalized to 100%. The activation energy (155 kJ/mol) and the diffusion constants were calculated from the 475° to 790°C temperature steps (tab. 5).

Table 5 shows that if a sample is heated to ~300°C for 1 Ma or more, argon loss is complete both in the newly formed illite and in the detrital mica. A temperature of around 300°C for 0.1 Ma produces an argon loss of around 80% in the detrital mica; at temperatures of 150°–200°C, argon loss is roughly an order

Table 5 Activation energies and diffusion parameters of the sample KAW 1804, 2–6 $\mu$ .

| loss<br>in | at | $D/a^2 = 1.2 \cdot 10^{-18} \text{ sec}^{-1}$<br>150° | $D/a^2 = 1.2 \cdot 10^{-15} \text{ sec}^{-1}$<br>200° | $D/a^2 = 1.2 \cdot 10^{-12} \text{ sec}^{-1}$<br>300° |
|------------|----|---|---|---|
| 10         | Ma | 14 %  | 98 %  | $\infty$  |
| 1          | Ma | 4 %   | 45 %  | $\infty$  |
| 0.1        | Ma | 1.5 %   | 14 %  | $\infty$  |

Calculated  $^{39}\text{Ar}$  loss in per cent for different diffusion coefficient of the newly formed illite with the calculated activation energy of 155 kJ/mol

| loss<br>in | at | $D/a^2 = 5.7 \cdot 10^{-20} \text{ sec}$<br>150° | $D/a^2 = 1.4 \cdot 10^{-17} \text{ sec}$<br>200° | $D/a^2 = 4.7 \cdot 10^{-16} \text{ sec}$<br>300° |
|------------|----|--|--|--|
| 10         | Ma | 0.9 %  | 15 %   | $\infty$   |
| 1          | Ma | 0.3 %  | 5 %  | $\infty$   |
| 0.1        | Ma | 0.09 %   | 1.5 %  | 81 %   |

Calculated  $^{39}\text{Ar}$  loss in per cent for different diffusion coefficient of the detrital mica component with the calculated activation energy of 183 kJ/mol

of magnitude lower. For the newly formed illite the Ar loss at 300°C is always 100% (supporting the closure temperature estimated by PURDY and JÄGER, 1976). If a temperature of 200°C for the illite over a period of 10 Ma is considered, the  $^{39}\text{Ar}$  loss is still 98%. If this temperature is maintained for only 0.1 Ma, the Ar loss in the illite is 14%, the same as for the  $^{40}\text{Ar}$  (rad) in the calculated model. From the calculated data the following geological model seems to be reasonable: a Tertiary metamorphism with temperature slightly below 300°C creates in the detrital mica a 90% Ar(rad) gas loss, during this time the newly formed illite loses all its radiogenic Ar. After a rapid cooling to a mean temperature of 150°C the subsequent slow cooling (10 Ma) produces a 14% Ar gas loss of the newly formed illite.

The slow cooling of the newly formed illite results in a small amount of gas loss (< 15%) as seen in the age spectrum. The point of inflection at about 45 Ma (transition from the convex to the concave curve in the age spectrum) provides a maximum age for the metamorphism in the Trias of Mauls.

As the above discussion shows the presence of a detrital component seriously disturbs the conventional K/Ar age of low grade metamorphism. In this study it was possible to distinguish between a detrital and a newly formed illite component, using the  $^{40}\text{Ar}/^{39}\text{Ar}$  method and a high resolution of temperature steps. If the relative age difference between the two components is very small it is possible that, from the superposition of the age spectra of old and new components, or by measuring too few temperature steps (see for example CHOPIN and MALUSKI, 1980) a quasi-plateau age is simulated at higher temperatures.

The following criteria for geologically meaningful plateau ages were stated by DALRYMPLE, LANPHERE and CLAGUE (p. 659, 1979). They are:

- 1) A well-defined, high temperature age spectrum plateau formed by three or more contiguous gas increments representing at least 50 per cent of the  $^{39}\text{Ar}$  released.
- 2) A well-defined isochron for plateau points; i.e. YORK 2 fit index SUMS/(N-2) ident with MSWD (mean square of weighted deviates) of less than 2.5 (BROOKS et al., 1972).
- 3) Concordant isochron ( $^{40}\text{Ar}/^{36}\text{Ar}$  versus  $^{40}\text{Ar}/^{39}\text{Ar}$  diagram) and plateau ages.
- 4) An  $^{40}\text{Ar}/^{36}\text{Ar}$  intercept on the isochron diagram not significantly different from the atmospheric value of 295.5 at 95% level of confidence.

If these criteria are not fulfilled, the data should be interpreted cautiously. It may be readily seen that the quasi-plateau like temperature range at 850°C does not agree with these demands.

### Geological Implications and Conclusions

The Permian and Triassic rocks of the so-called Trias of Maultal underwent a metamorphism at the beginning of lower greenschist facies grade as demonstrated by the crystallinity index of about 4 for the illite. The  $2M_1$  polymorphs of the investigated illites point to the complete transition from diagenetic stage (1M/1Md) to the metamorphic stage (2M). Illites of phengitic composition are also well known from other metapelites in metamorphic profiles (see FREY, 1978; E. FRANK, 1980). X-ray analyses show no evidence of a detrital mica component in the grain size fraction investigated from the Trias of Maultal.

The age spectrum shows that the metamorphic temperatures of the lower greenschist facies were insufficient to completely reset the ages of the micas. Two phases can be recognized: a newly formed illite, which has lost 15% of its radiogenic argon by cooling since its formation approximately 45 Ma ago (that means a maximum age for the alpine metamorphism), and a mica component with a minimum age of 200 Ma. This age provides a minimum age for the detrital component whether it is the time of sedimentation or of diagenesis. This older component could represent the innermost part (nucleus of crystallisation) of newly formed illite or separate grains. The amount of this old mica component cannot be greater than 5%.

A calculated model of such a mixture shows that a 5% contribution of the old component does not seriously disturb the age spectrum in the lower temperature range. At higher temperatures the influence of the older mica becomes dominant, explaining the rapid increase in the apparent age.

The apparent ages up to 200 Ma obtained for the high temperature steps indicates that the 80 Ma phase (SATIR, 1975) seen in the Austroalpine basement did not affect the Permian sediments sufficiently to completely reset the age of the detrital component. The newly formed illites were open systems during the Tauern metamorphism. The metamorphism of the Trias of Maultal cannot be older than 45 Ma, as indicated by the point of inflection on figure 3. The subsequent slow cooling is demonstrated by the argon loss (15%) in the low temperature steps.

The surprisingly low conventional K/Ar ages (15–22 Ma) in the Trias of Stilfser, the southwestern continuation of the Trias of Maultal, were interpreted as cooling ages by W. FRANK, et al. (1977). Such an interpretation implies a higher metamorphic influence of the Tertiary metamorphism in the Trias of Stilfser than in the Trias of Maultal.

As with many other studies, this work was also carried out to test whether geochronological data may help in deciding to which unit a rock succession belongs. As mentioned above the Trias of Maultal is situated in the Austroalpine basement, and only the northern block of this basement was influenced by the alpidic Tertiary metamorphism and tectonism. From the evidence of mineral-

ological and petrological studies (STOECKHERT, 1982) and the biotite Rb/Sr and K/Ar cooling ages (BORSI et al., 1978; HAMMERSCHMIDT, 1981) the alpidic temperature of the northern block was too high to give an age pattern consistent with that found in this study. It is therefore improbable that the Trias of Mauls belongs to this northern basement block.

As the Trias of Mauls is situated at the border of the northern and the southern block of the Austroalpine basement, it is proposed that during the rapid uplift along the DAV line (STOECKHERT, 1982), the alpine metamorphosed northern block was uplifted into a position besides the unmetamorphosed Trias of Mauls. Juxtaposition of the heated basement against the relatively cool mesozoic pile was sufficient to heat the Trias of Mauls to the beginning of the greenschist facies metamorphic conditions.

#### Acknowledgements

I wish to thank Frau Prof. E. Jäger for her suggestions and critical reading of this manuscript. I am grateful to Dr. A.J. Hurford for his comments and assistance with the English. Dr. J.C. Hunziker and Dr. E. Frank critically commented a former version. Mr R. Siegenthaler, Mr M. Flisch and Dr. U. Aschliman supported this work with their advice on programming and Ar analyses. For the use of the mass spectrometer equipment at the Physikalisches Institut in Bern I am indebted to Prof. P. Eberhardt and Prof. J. Geiss.

Financial support was provided by Schweizerischer Nationalfonds zur Förderung der wissenschaftlichen Forschung and Deutscher Akademischer Austauschdienst.

The manuscript was reviewed by Prof. P. Eberhardt, Bern, Dr. R. Hänni, Basel, and Prof. G. Nollau, Erlangen.

#### References

- BESANG, C., HARRE, W., KARL, F., KREUZER, H., LENZ, H., MÜLLER, P. und WENDT, I. (1968): Radiometrische Altersbestimmungen (Rb/Sr und K/Ar) an Gesteinen des Venediger-Gebietes (Hohe Tauern, Österreich). *Geol. Jb.*, v. 86, p. 835–844.
- BORSI, S., DEL MORO, A. e FERRARA, G. (1972): Eta radiometriche delle rocce intrusive del Massiccio di Bressanone–Ivigna–Monte Croce (Alto Adige). *Boll. Soc. Geol. It.*, 91, p. 387–406.
- BORSI, S., DEL MORO, A., SASSI, F. P. and ZIRPOLI, G. (1973): Metamorphic evaluation of the austroalpine rocks to the south of the Tauern window (Eastern Alps): Radiometric and geopetrologic data. *Mem. Soc. Geol. Ital.*, v. 12, p. 549–571, Pisa.
- BORSI, S., DEL MORO, A., SASSI, F. P., ZANFERRARI, A. and ZIRPOLI, G. (1978): New geopetrologic and radiometric data on the alpine history of the austroalpine continental margin south of the Tauern window (Eastern Alps). *Mem. Soc. Geol.*, v. XXXII, p. 3–17, Padova.
- BROOKS, C., HART, S. R. and WENDT, I. (1972): Realistic use of two error regression treatments as applied to rubidium strontium data. *Rev. Geophys. Space Phys.*, v. 10, p. 551–557.
- BURNHAM, C. and RADOSLOVICH, E. (1964): Crystal structures of coexisting muscovite and paragonite. *Carn. Inst. Year Book*, p. 232–236.
- CHOPIN, C. and MALUSKI, H. (1980):  $^{40}\text{Ar}/^{39}\text{Ar}$  dating of high pressure metamorphic micas from the Gran Paradiso Area (Western Alps): Evidence against the blocking temperature Concept. *Contr. Min. Petr.*, v. 74, 109–122.

- DALRYMPLE, B. G., LANPHERE, M. A. and CLAGUE, D. A. (1979): Conventional and  $^{40}\text{Ar}/^{39}\text{Ar}$  K-Ar ages of volcanic rocks from Ojin (Site 430), Nintoku (Site 432) and Suiko (Site 433) seamounts and the chronology of volcanic propagation along the Hawaiian-Emperor chain. Initial Report of Deep Sea Drilling Project, Vol. LV., 1979.
- DUNOYER DE SEGNOZAC, G. (1970): The transformation of clay minerals during diagenesis and low grade metamorphism: a review, *Sedimentology*, 15, p. 281–346, 1970.
- FRANK, E. (1979): Metamorphose mesozoischer Gesteine im Querprofil Brig–Verampio: Mineralogisch-petrographische und isotopengeologische Untersuchungen, 204 pp. unveröffentl. Dissertation, Bern.
- FRANK, E. and STETTLER, A. (1979): K-Ar and  $^{39}\text{Ar}/^{40}\text{Ar}$  systematics of white-mica from an alpine metamorphic profile in the Swiss Alps. *Schweiz. Min. Petr. Mitt.*, 59, 3, p. 375–394, Basel 1979.
- FRANK, W., ALBER, J. und THÖNI, M. (1977): Jungalpine K/Ar Alter von Hellglimmern aus dem Permotriaszug von Maults-Penser Joch (Südtirol). *Anz. math.-natw.. Kl. der Österr. Akad. der Wiss.* Jg. 1977, Nr. 7, 6 Seiten, Wien 1977.
- GÜVEN, N. (1971): The crystal structures of  $2M_1$  phengites and  $2M_1$  muscovites. *Zeitschr. Krist.*, v. 134, p. 196–212.
- GUGGISBERG, S. (1977): Absolute Chronologie der Marebildung auf dem Mond. Unveröffentl. Dissertation Bern.
- HAMMERSCHMIDT, K. (1980): Querprofil über den Tauernsüdrand: Petrographie, Tektonik und Geochronologie von der Schieferhülle zur Matreier Zone und dem Oberostalpinen Altkristallin bis zum Rieserferner, Südtirol (Alto Adige). Unveröff. Diss. Universität Bern, 1980.
- HAMMERSCHMIDT, K. (1981): Isotopengeologische Untersuchungen am Augengneis von Typ Campo Tures bei Rain in Taufers, Südtirol. *Mem. di Sci. Geol.*, Vol. XXXIV, p. 273–300, Padova 1981.
- HARRISON, T. M. and McDUGALL, I. (1980): Investigation of intrusive contact, northwest Nelson, New Zealand-II. Diffusion of radiogenic and excess Ar in hornblende revealed by  $^{40}\text{Ar}/^{39}\text{Ar}$  age spectrum analysis. *Geochim. Cosmochim. Acta*, Vol. 44, p. 2005–2020, 1980.
- HOWER, J., ESSLINGER, E. V., HOWER, M. E. and PERRY, E. A. (1976): The mechanism of burial metamorphism of argillaceous sediments. *Geol. Soc. Am. Bull.*, 87, 1976.
- HUNECKE, J. C. and SMITH, S. P. (1976): The realities of recoil: Ar recoil out of small grains and anomalous age patterns in  $^{40}\text{Ar}/^{39}\text{Ar}$  dating. *Proc. Lunar Sci. Conf. 7th., Suppl. Geochim. Cosmochim.*, p. 1987–2008, 1976.
- HUNZIKER, J. C. (1974): Rb/Sr and K/Ar age determination and the alpine tectonic history of the western alps. *Mem. Ist. Geol. Min. Univ. Padova*, v. XXXI, 55 pp.
- HUNZIKER, J. C. (1979): in: JÄGER, E. and HUNZIKER, J. C., ed. (1979): *Lectures in isotopic geology*, Springer Verlag, Heidelberg.
- HURLEY, P. M., BROOKINS, D. G., PINSON, W. H., HART, S. P. and FAIRBAIRN, H. W. (1966): Ar age studies of Mississippi and other river sediments. *Bull. Geol. Am.* 72, 1807.
- HURLEY, P. M. in: SCHAEFFER, O. A. und ZÄHRINGER, J. (eds.), (1966): *Potassium Argon Dating*, Springer Verlag.
- JÄGER, E., KARL, F. und SCHMIDEGG, O. (1969): Rubidium-Strontium-Altersbestimmungen an Biotit-Muskovit-Granitgneisen (Typus Augen-Flaserigneise) aus dem nördlichen Grossvenedigerbereich (Hohe Tauern). *Tscherm. Min. Petr. Mitt.*, v. 13, p. 251–254.
- KÜBLER, B. (1967): La cristallinité de l'illite et les zones tout a fait superieures du metamorphisme. *Etages Tectoniques*, p. 105–122, Colloque à Neuchâtel, 1967.
- LANPHERE, M. A. and DALRYMPLE, G. B. (1976): Identification of excess  $^{40}\text{Ar}$  by the  $^{40}\text{Ar}/^{39}\text{Ar}$  age spectrum technique. *Earth Planet. Sci. Lett.*, v. 32, p. 141–148, Amsterdam.
- MAURER, P. (1973):  $^{40}\text{Ar}/^{39}\text{Ar}$ -Kristallisationsalter und  $^{37}\text{Ar}/^{38}\text{Ar}$ -Strahlungsalter von Apollo 11-, 12- und 17-Steinen und dem Apollo 17-“orange soil”. Unveröffentl. Liz.-Arbeit, Bern 1973.
- ODIN, G. S. (1982): *Numerical dating in stratigraphy*, Wiley and Sons Ltd. in press.

- PURDY, J. (1972): The Varian Mat GD 150 for Argon Analyses in connections with K/Ar dating. *Ecl. Helv.*, v. 65, p. 317–320, Basel.
- PURDY, J. and JÄGER, E. (1976): K/Ar ages on rock-forming minerals from the Central Alps. *Mem. Ist. Geol. Min. Univ. Padova*, v. XXX, 32 p.
- RADOSLOVICH, E. W. (1960): The structure of muscovite  $\text{KAl}_2(\text{Si}_3\text{Al})\text{O}_{10}(\text{OH})_2$ . *Acta Crystallogr.*, v. 13, p. 919–932.
- SATIR, M. (1975): Die Entwicklungsgeschichte der westlichen Hohen Tauern und der südlichen Ötztalmasse auf Grund radiometrischer Altersbestimmungen. *Mem. Ist. Geol. Min. Univ. Padova*, v. XXX, 82 pp., Padova.
- SCHINDLMAYR, W.-E. (1968): Geologische Untersuchungen in der Umgebung von Mauls und Stilfes in Südtirol, 113 p., München 1968.
- SCHWARZMÜLLER, J. (1970): Ein Edelgasanalysensystem mit automatischer Datenerfassung und Edelgasmessungen an Strukturelementen des Apollo 11 Mondstaubes, unveröff. Dissertation Universität Bern.
- STETTLER, A., EBERHARD, P., GEISS, J., GRÖGLER, N. and MAURER, P. (1973):  $^{39}\text{Ar}/^{40}\text{Ar}$  ages and  $^{37}\text{Ar}/^{38}\text{Ar}$  exposure ages of lunar rocks. *Proc. IV. Lun. Sci. Conf. (Suppl. IV, Geochim. and Cosmochim. Acta)* Vol. 2, p. 1865–1888.
- STOECKHERT, B. (1982): Deformation und retrograde Metamorphose im Altkristallin südlich des westlichen Tauernfensters Südtirol. Dissertation Universität Erlangen, Eigenverlag, Erlangen.
- TURNER, G. (1968): The distribution of potassium and argon in chondrites. In: *Origin and Distribution of the Elements*. AHRENDT (ed.), London.
- TURNER, G., CADOGAN, P. H. and YONGE, C. J. (1973): Argon selenochronology. *Proc. IV. Lun. Sci. Conf. (Suppl. IV, Geochim. and Cosmochim. Acta)* Vol. 2, p. 1889–1914.
- YODER, H. S. and EUGSTER, H. P. (1955): Synthetic and natural muscovites. *Geochim. Cosmochim. Acta*, 8, p. 225–280, 1955.
- ZEN, E.-AN, ALBEE, A. L. (1964): Coexisting muscovite and paragonite in pelitic schists. *Am. Min.*, v. 49, p. 904–925.